

3-17-2023

Adaptive Modified RISE-based Quadrotor Trajectory Tracking with Actuator Uncertainty Compensation

Emmanuel Ogbanje Ijoga
Embry-Riddle Aeronautical University

William MacKunis
Embry-Riddle Aeronautical University - Daytona Beach, mackuniw@erau.edu

Krishna Bhavithavya Kidambi
University of Dayton

Madhur Tiwari
Florida Institute of Technology

Follow this and additional works at: <https://commons.erau.edu/publication>



Part of the [Aeronautical Vehicles Commons](#)

Scholarly Commons Citation

Ijoga, E. O., MacKunis, W., Kidambi, K. B., & Tiwari, M. (2023). Adaptive Modified RISE-based Quadrotor Trajectory Tracking with Actuator Uncertainty Compensation. *Electrical Engineering and Systems Science*, (). <https://doi.org/10.48550/arXiv.2303.10270>

This Article is brought to you for free and open access by Scholarly Commons. It has been accepted for inclusion in Publications by an authorized administrator of Scholarly Commons. For more information, please contact commons@erau.edu.

Adaptive Modified RISE-based Quadrotor Trajectory Tracking with Actuator Uncertainty Compensation

Krishna Bhavithavya Kidambi¹, Madhur Tiwari², Emmanuel Ogbanje Ijoga³ and William MacKunis⁴

Abstract—This paper presents an adaptive robust nonlinear control method, which achieves reliable trajectory tracking control for a quadrotor unmanned aerial vehicle in the presence of gyroscopic effects, rotor dynamics, and external disturbances. Through novel mathematical manipulation in the error system development, the quadrotor dynamics are expressed in a control-oriented form, which explicitly incorporates the uncertainty in the gyroscopic term and control actuation term. An adaptive robust nonlinear control law is then designed to stabilize both the position and attitude loops of the quadrotor system. A rigorous Lyapunov-based analysis is utilized to prove asymptotic trajectory tracking, where the region of convergence can be made arbitrarily large through judicious control gain selection. Moreover, the stability analysis formally addresses gyroscopic effects and actuator uncertainty. To illustrate the performance of the control law, comparative numerical simulation results are provided, which demonstrate the improved closed-loop performance achieved under varying levels of parametric uncertainty and disturbance magnitudes.

I. INTRODUCTION

Unmanned aerial vehicles (UAVs) (or Quadrotors) have the potential to transport people and things to locations not traditionally served by current modes of air transportation. The UAV market can potentially proliferate, and one can sense that the lack of regulation is currently preventing this. Hundreds of exciting and promising applications in various domains such as air delivery, surveying, agriculture, architecture, security, and video entertainment are being developed [1], [2].

Developing reliable and safe control algorithms is still a challenging task in a myriad of quadrotor control applications [3]. Over the last decade several methods have been proposed to compensate for uncertain and time-varying external operating conditions; however, there remain numerous open challenges in the design of robust and adaptive nonlinear quadrotor UAV control systems, which are rigorously proven to simultaneously compensate for external disturbances (e.g., due wind gusts and aerodynamic anomalies) and internal anomalies, disturbances, and unmodeled effects in the UAV actuation dynamics (e.g., due to electromechanical propeller motor dynamics and/or actuator faults).

Numerous recent approaches to quadrotor control are based on classical control methods applied to linearized models of the UAV dynamics [4], [5], [6], [7]. Popular linear control methods include proportional-integral-derivative (PID) control [6] and linear quadratic regulators (LQR) [7]. While PID and LQR methods benefit from simple implementation and intuitive control gain-tuning, they have limited capability to compensate for the inherent nonlinearities in the quadrotor dynamics; and they tend to have low robustness to external disturbances.

In an effort to overcome the limitations of linear control methods, nonlinear control techniques have been widely shown to achieve an increased level of reliability in quadrotor flight under various uncertain and adversarial operating conditions. Common nonlinear control design approaches include feedback linearization [8], [9], backstepping [10], [11], [12], adaptive control [13], [14] and robust control [15], [16], [17]. Advantages to feedback linearization include mathematical simplicity and easy implementation; however, they often incur reduced robustness to disturbances and sensitivity to model uncertainty. To address this, feedback linearization-based linear control designs often employ robust nonlinear compensators to achieve the desired disturbance-rejection objectives [9]. The authors in [12] present an adaptive backstepping controller to track time-varying trajectories with parameter uncertainties and under-actuation. The control algorithm is extended to include velocity input and motor coefficients, and geometric parameters are handled by the adaptive laws.

In [15], a robust control scheme based on nonlinear dynamic inversion (NDI) for disturbance rejection is proposed. However, to achieve performance in agile quadcopters, accounting for actuator uncertainty is vital. The authors in [18] develop an agile control subjected to aerodynamic drag, the center of gravity shift, and motor dynamics. It is shown that accounting for uncertainties in the actuator dynamics is essential to achieve the desired trajectory-tracking performance.

While standard sliding mode control approaches are widely known for their disturbance-rejection capabilities, their implementation can be challenging due to the use of high-bandwidth switching [19], [20]. Motivated by this, robust integral of the sign of the error (RISE)-based control can be used to achieve reliable disturbance rejection using continuous control [21]. RISE has been widely shown to achieve superior rejection of norm-bounded disturbances in various recent results [22], [23], [24]. In addition, our recent result in [25] presents a modified RISE (MRISE)-based

¹Krishna Bhavithavya Kidambi is an Assistant Professor in the Department of Mechanical and Aerospace Engineering, University of Dayton, Dayton, OH 45469. kkidamb1@udayton.edu

²Madhur Tiwari is an Assistant Professor in the Department of Aerospace, Physics and Space Sciences, Florida Institute of Technology, Melbourne, FL 32901. mtiwari1@fit.edu

³Emmanuel Ogbanje Ijoga, William MacKunis are with Physical Sciences Department, Embry-Riddle Aeronautical University, Daytona Beach, FL 32114. ijogae@my.erau.edu, mackuniw@erau.edu

quadrotor control design, which is proven to reject external disturbances of varying magnitudes and compensate for varying levels of parametric uncertainty in the UAV dynamics. While the MRISE result achieved significant performance improvement in trajectory tracking compared to traditional RISE, the work does not formally incorporate the effects of actuator uncertainty and gyroscopic effects in the quadrotor dynamic model.

Motivated by this and future demands of building robust and agile quadrotors, we propose an adaptive MRISE-based trajectory tracking control method for a quadrotor system subjected to parametric uncertainty and unmodeled gyroscopic effects and uncertainties in the actuator dynamics in addition to external disturbances. The result is achieved through a non-trivial reworking of the error system development and stability analysis in [25], which now formally incorporates unmodeled effects in the actuation dynamic model. The primary contributions of this result can be summarized as follows:

- 1) An augmented adaptive MRISE control design for both the inner and outer loop of the quadrotor tracking control system, which formally incorporates feedback compensators for the actuator uncertainty, gyroscopic effects, model uncertainties and external disturbances. The control algorithm accounts for varying magnitudes of uncertainty ($\pm 15\%$) with little or no gain tuning.
- 2) A rigorous closed-loop stability analysis using a Lyapunov-based approach, which provides a detailed derivation of semi-global asymptotic tracking and the specific control gain conditions under which convergence can be guaranteed.
- 3) A detailed comparative numerical simulation study to demonstrate the performance of the proposed control design.

The rest of the paper is organized as follows: Section II describes the nonlinear dynamic model of the quadrotor, especially Section II-C describes a detailed model incorporating the gyroscopic effects and the actuator dynamics. The open-loop and closed-loop error systems are described in Section III-A and III-B, respectively. In Section IV, the closed-loop stability analysis is presented. Finally, Section V presents the numerical simulations to demonstrate the effectiveness of the proposed method, followed by conclusions in Section VI.

II. MATHEMATICAL MODEL

A. Quad Dynamics

The mathematical model of quadrotor dynamics is well studied in the literature [26], [27]. The explicit form of the dynamics by using the Newton–Euler method with position and orientation can be written as [28]

$$m\dot{V} = F_g + F_T + F_d + d_1(t) \quad (1a)$$

$$I\dot{\Omega} = -\Omega \times I\Omega + \tau - \tau_a + \tau_g + d_2(t) \quad (1b)$$

where $m \in \mathbb{R}^+$ is the mass of the quadrotor, $V = [V_x, V_y, V_z]^T$ and $\Omega = [p, q, r]^T$ denote the translational and angular velocity defined in the inertial frame and body

frame, respectively. $I = \text{diag}(I_x, I_y, I_z) \in \mathbb{R}^{3 \times 3}$ is a positive definite diagonal moment of inertia matrix, and $d_1(t), d_2(t)$ are the external disturbances in the translation and rotational dynamics respectively.

The remaining forces in the translational dynamics are given as $F_g = [0, 0, -mg]^T$, where $g = 9.81 \frac{m}{s^2}$ is the gravitational acceleration. F_d is the drag due to the translational motion and is given by

$$F_d = -\text{diag}(K_{d_x}, K_{d_y}, K_{d_z})V \quad (2)$$

where $K_{d_x}, K_{d_y}, K_{d_z}$ are translational drag coefficients. The control input $F_T \in \mathbb{R}$ is the total thrust generated by all four motors and is given as

$$F_T = R_1 \sum_{i=1}^4 F_i \quad (3)$$

where $F_i = K_T u_i^2$, and K_T is the thrust coefficient and u_i is the speed of i^{th} motor. The term R_1 is given as

$$R_1 = \begin{bmatrix} \cos(\psi) \sin(\theta) \cos(\phi) + \sin(\psi) \sin(\phi) \\ \sin(\phi) \sin(\theta) \sin(\psi) - \cos(\psi) \sin(\phi) \\ \cos(\theta) \cos(\phi) \end{bmatrix} \quad (4)$$

The gyroscopic torque τ_g is given as

$$\tau_g = \sum_{i=1}^4 \Omega \times I_r \begin{bmatrix} 0 \\ 0 \\ (-1)^{i-1} u_i \end{bmatrix} \quad (5)$$

where I_r is the rotor inertia. The aerodynamic frictional torque τ_a is given as

$$\tau_a = -\text{diag}(K_{a_x}, K_{a_y}, K_{a_z}) \|\Omega\|^2 \quad (6)$$

where $K_{a_x}, K_{a_y}, K_{a_z}$ are the coefficients of aerodynamic friction. The torque τ applied on the quadrotor is given by

$$\tau = \begin{bmatrix} \tau_\phi \\ \tau_\theta \\ \tau_\psi \end{bmatrix} = \begin{bmatrix} 0 & -lK_T & 0 & lK_T \\ lK_T & 0 & -lK_T & 0 \\ K_D & -K_D & K_D & -K_D \end{bmatrix} \begin{bmatrix} u_1^2 \\ u_2^2 \\ u_3^2 \\ u_4^2 \end{bmatrix} \quad (7)$$

where $\tau_\phi, \tau_\theta, \tau_\psi$ denotes the torque along x, y, z axis respectively, l is the distance between each rotor to the quadrotor center of mass, and K_D is the drag coefficient.

B. Actuator Dynamics

The control input commands to the quadrotor are applied through a DC motor and when tracking aggressive trajectories, actuator dynamics cannot be ignored for the sake of precise tracking performance. The dynamics of the i^{th} motor speed is given as [18]

$$\dot{u}_i = \frac{k_\tau}{I_r} (u_{ci} - u_i) \quad (8)$$

where k_τ is the motor coefficient and u_{ci} is the commanded speed of the i^{th} motor and u_i is introduced in (3).

C. Uncertain Quadrotor Model

The dynamic equations in (1) are recast by incorporating parametric and actuator uncertainties and are simplified as

$$\dot{P} = V \quad (9a)$$

$$\dot{V} = f_1(V) + F_V + \Delta_V F_V + d_V(t) \quad (9b)$$

$$\dot{\omega} = \Omega \quad (9c)$$

$$\dot{\Omega} = f_2(\Omega) + \tau_\Omega + \Delta_\Omega \tau_\Omega + d_\Omega(t) \quad (9d)$$

where $P = [x, y, z]^T$, $V = [V_x, V_y, V_z]^T$, $\omega = [\phi, \theta, \psi]^T$ and $\Omega = [p, q, r]^T$ are the position, velocity, angular position and angular velocity in 3-D; and the following definitions have been made:

$$F_V = \frac{F_T}{m}; \quad \Delta_V F_V = \frac{R_1}{m} \sum_{i=1}^4 \Delta F_i$$

$$f_1(V) = \frac{\bar{F}_g}{m} + \frac{\bar{F}_d}{m}$$

$$d_V(t) = -\frac{\Delta m \dot{V}}{m} + \frac{\Delta F_g}{m} + \frac{\Delta F_d}{m} + \frac{d_1(t)}{m}$$

$$\tau_\Omega = R_2 \times [u_1^2, u_2^2, u_3^2, u_4^2]^T$$

$$\Delta_\Omega \tau_\Omega = \Delta R_2 \times [u_1^2, u_2^2, u_3^2, u_4^2]^T$$

$$f_2(\Omega) = I^{-1} \left[-\overline{\Omega \times I \Omega} - \bar{\tau}_a + \bar{\tau}_g \right]$$

$$d_\Omega(t) = I^{-1} \left[-\overline{\Omega \times \Delta I \Omega} - \Delta I \dot{\Omega} - \Delta \tau_a + \Delta \tau_g + d_2(t) \right]$$

III. CONTROL MODEL

The control objective is to design the control signal to regulate the quadrotor states to a given desired time-varying reference trajectory that is sufficiently smooth, despite the presence of uncertainties in the dynamic and actuator model respectively. Thus, the control objective can be mathematically stated as

$$\|\xi(t)\| \rightarrow 0 \quad (10)$$

where ξ in (10) is the difference between the current state and desired state of the quadrotor and $\|\cdot\|$ in (10) denotes standard Euclidean norm.

Assumption 1: The desired trajectory profile $P_d(t)$ and its first three-time derivatives are bounded in the sense that $P_d(t), \dot{P}_d(t), \ddot{P}_d(t), \dddot{P}_d(t) \in \mathcal{L}_\infty \forall t \geq 0$.

Assumption 2: The disturbances in the quadrotor dynamics in (9b) and (9d) are smooth enough such that

$$\|\dot{d}_V\| \leq \epsilon_1, \quad \|\dot{d}_\Omega\| \leq \epsilon_2 \quad (11)$$

where ϵ_1, ϵ_2 are some unknown positive constants.

A. Open-loop Error System

1) *Position Loop:* To assess the controller performance and to enable the subsequent stability analysis, the tracking error $\xi_1(t) \in \mathbb{R}^3$ and auxiliary tracking errors $\xi_2(t), \eta_1(t) \in \mathbb{R}^3$ for the position loop are defined as

$$\xi_1 = P - P_d, \quad (12)$$

$$\xi_2 = \dot{\xi}_1 + k_1 \xi_1 = V - V_d^* \quad (13)$$

$$V_d^* = V_d - k_1 \xi_1 \quad (14)$$

$$\eta_1 = \dot{\xi}_2 + k_2 \xi_2 \quad (15)$$

where $P_d = [x_d, y_d, z_d]^T \in \mathbb{R}^3$, $V_d = [V_{d_x}, V_{d_y}, V_{d_z}]^T \in \mathbb{R}^3$ are the desired position and velocity; and $k_1, k_2 \in \mathbb{R}$ denote positive control gains. Taking the derivative of (15) and using the definition in (12) and (13) the open loop error dynamics can be expressed as

$$\dot{\eta}_1 = \ddot{V} - \ddot{V}_d + k_1(\dot{\xi}_2 - k_1 \dot{\xi}_1) + k_2 \dot{\xi}_2 \quad (16)$$

By using the definition in (9b) the tracking error in (16) is expanded as

$$\begin{aligned} \dot{\eta}_1 &= \dot{f}_1(V) + \dot{F}_V(t) + \dot{\Delta}_V F_V(t) + \dot{d}_V(t) - \ddot{V}_d \\ &+ k_1(\dot{\xi}_2 - k_1 \dot{\xi}_1) + k_2 \dot{\xi}_2. \end{aligned} \quad (17)$$

The error dynamics in (17) can be expressed as

$$\dot{\eta}_1 = \tilde{\Gamma}_1 + \Gamma_{1d} + \dot{F}_V(t) + \dot{\Delta}_V F_V(t) - \xi_2 \quad (18)$$

where the unknown auxiliary functions, $\tilde{\Gamma}_1(t), \Gamma_{1d}(t) \in \mathbb{R}^3$ are defined as

$$\tilde{\Gamma}_1(t) = \dot{f}_1(V) + k_1(\dot{\xi}_2 - k_1 \dot{\xi}_1) + k_2 \dot{\xi}_2 + \xi_2 \quad (19)$$

$$\Gamma_{1d} = \dot{d}_V(t) - \ddot{V}_d. \quad (20)$$

Assumption 3: Approximate model knowledge is available such that $\dot{\Delta}_V(t)$ satisfies

$$\left\| \dot{\Delta}_V(t) \right\|_{i_\infty} < \delta_1 < 1, \quad (21)$$

where $\delta_1 \in \mathbb{R}^+$ is a known bounding constant, and $\|\cdot\|_{i_\infty}$ denotes the induced infinity norm.

The motivation for the separation of terms in (19) and (20) is based on the fact that the following inequalities can be developed

$$\|\tilde{\Gamma}_1\| \leq \rho_1 (\|\mu_1\|) \|\mu_1\|, \quad \|\Gamma_{1d}\| \leq \kappa_{\Gamma_{1d}}, \quad \|\dot{\Gamma}_{1d}\| \leq \kappa_{\dot{\Gamma}_{1d}} \quad (22)$$

where $\kappa_{\Gamma_{1d}}, \kappa_{\dot{\Gamma}_{1d}} \in \mathbb{R}^+$ are known bounding constants; $\rho(\cdot)$ is a positive, globally invertible, non-decreasing function; and $\mu_1(t) \in \mathbb{R}^9$ is defined as

$$\mu_1(t) \triangleq \left[\xi_1^T(t) \quad \xi_2^T(t) \quad \eta_1^T(t) \right]^T. \quad (23)$$

2) *Attitude Loop:* The tracking error in the attitude loop $\xi_3(t) \in \mathbb{R}^3$ and auxiliary tracking errors $\xi_4(t), \eta_2(t) \in \mathbb{R}^3$ are defined as

$$\xi_3 = \omega - \omega_d, \quad (24)$$

$$\xi_4 = \dot{\xi}_3 + k_3 \xi_3 = \Omega - \Omega_d^* \quad (25)$$

$$\Omega_d^* = \Omega_d - k_3 \xi_3 \quad (26)$$

$$\eta_2 = \dot{\xi}_4 + k_4 \xi_4 \quad (27)$$

where $\omega_d = [\phi_d, \theta_d, \psi_d]^T \in \mathbb{R}^3$, $\Omega_d = [p_d, q_d, r_d]^T \in \mathbb{R}^3$ are the desired angular position and angular velocity, $k_3, k_4 \in \mathbb{R}$ denote positive control gains.

Since the quadrotor is an underactuated system with 4 control inputs and 6 outputs and using the differential flatness property, the control input can be obtained from four flat outputs $[x_d, y_d, z_d, \psi_d]^T$ (user-defined). In addition, the desired trajectories of roll (ϕ_d) and pitch (θ_d) depend on

these flat outputs and are defined according to the dynamics (9a) and (9b) as [12], [24]:

$$\phi_d = \sin^{-1} \left[\frac{m}{U_1} (U_1 \sin(\psi_d) - U_2 \cos(\psi_d)) \right], \quad (28)$$

$$\theta_d = \tan^{-1} \left[\frac{1}{U_3} (U_1 \cos(\psi_d) + U_2 \cos(\psi_d)) \right], \quad (29)$$

where F_V is the thrust force, which is defined as

$$F_V = m \sqrt{U_1^2 + U_2^2 + U_3^2} \quad (30)$$

where $U_i = F_V \times R_1(i)$ for $i = 1, 2, 3$ and $R_1(i)$ is the i^{th} row of matrix R_1 defined in (49).

By taking the derivative of (27) and using the definition in (24) and (25) the open loop error dynamics in the attitude loop can be expressed as

$$\dot{\eta}_2 = \ddot{\Omega} - \ddot{\Omega}_d + k_3(\dot{\xi}_4 - k_3\dot{\xi}_3) + k_4\dot{\xi}_4 \quad (31)$$

By using the definition in (9d) the tracking error in (31) is expanded as

$$\begin{aligned} \dot{\eta}_2 &= \dot{f}_2(\Omega) + \dot{\tau}_\Omega(t) + \dot{\Delta}_\Omega \tau_\Omega(t) + \dot{d}_\Omega(t) - \ddot{\Omega}_d \\ &+ k_3(\dot{\xi}_4 - k_3\dot{\xi}_3) + k_4\dot{\xi}_4. \end{aligned} \quad (32)$$

The error dynamics in (32) can be expressed as

$$\dot{\eta}_2 = \tilde{\Gamma}_2 + \Gamma_{2d} + \dot{\tau}_\Omega(t) + \dot{\Delta}_\Omega \tau_\Omega(t) - \xi_4 \quad (33)$$

where the unknown auxiliary functions, $\tilde{\Gamma}_2(t), \Gamma_{2d}(t) \in \mathbb{R}^3$ are defined as

$$\tilde{\Gamma}_2(t) = \dot{f}_2(\Omega) + k_3(\dot{\xi}_4 - k_3\dot{\xi}_3) + k_4\dot{\xi}_4 + \xi_4 \quad (34)$$

$$\Gamma_{1d} = \dot{d}_\Omega(t) - \ddot{\Omega}_d. \quad (35)$$

Assumption 4: Approximate model knowledge is available such that $\dot{\Delta}_\Omega(t)$ satisfies

$$\left\| \dot{\Delta}_\Omega(t) \right\|_{i\infty} < \delta_2 < 1, \quad (36)$$

where $\delta_2 \in \mathbb{R}^+$ is a known bounding constant, and $\|\cdot\|_{i\infty}$ denotes the induced infinity norm.

The motivation for the separation of terms in (34) and (35) are based on the fact that the following inequalities can be developed

$$\|\tilde{\Gamma}_2\| \leq \rho_2 (\|\mu_2\|) \|\mu_2\|, \|\Gamma_{2d}\| \leq \kappa_{\Gamma_{2d}}, \|\dot{\Gamma}_{2d}\| \leq \kappa_{\dot{\Gamma}_{2d}} \quad (37)$$

where $\kappa_{\Gamma_{2d}}, \kappa_{\dot{\Gamma}_{2d}} \in \mathbb{R}^+$ are known bounding constants; $\rho(\cdot)$ is a positive, globally invertible, non-decreasing function; and $\mu_2(t) \in \mathbb{R}^9$ is defined as

$$\mu_2(t) \triangleq \begin{bmatrix} \xi_3^T(t) & \xi_4^T(t) & \eta_2^T(t) \end{bmatrix}^T. \quad (38)$$

B. Closed-loop Error System

1) *Position Loop:* Based on the open-loop error system dynamics in (18), the control term $F_V(t)$ is designed as:

$$\begin{aligned} \dot{F}_V(t) &= -\alpha_F \|F_V(t)\| \text{sgn}(\eta_1) - (\alpha_1 + 1)\eta_1 \\ &\quad - \hat{\lambda}_1 \text{sgn}(\eta_1), \end{aligned} \quad (39)$$

where $\alpha_F, \alpha_1 \in \mathbb{R}$ are positive, control gains. $\hat{\lambda}_1 \in \mathbb{R}^3$ is a adaptive nonlinear feedback gain, which is defined as

$$\dot{\hat{\lambda}}_{1i} = \beta_1 \text{sgn}(\eta_1) \eta_1 \quad (40)$$

where $i = 1, 2, 3$, β_1 is a positive adaptation gain.

Remark 1: Note that the theoretical design and stability analysis in this paper are based on the discontinuous signum function, i.e.,

$$\text{sgn}(\sigma) = \begin{cases} 1 & \sigma > 0 \\ 0 & \sigma = 0 \\ -1 & \sigma < 0 \end{cases} \quad \forall \sigma \in \mathbb{R}. \quad (41)$$

After substituting (39) into (18), the closed-loop error dynamics is obtained as

$$\begin{aligned} \dot{\eta}_1 &= \tilde{\Gamma}_1 + \Gamma_{1d} - \alpha_F \|F_V(t)\| \text{sgn}(\eta_1) - (\alpha_1 + 1)\eta_1 \\ &\quad - \hat{\lambda}_1 \text{sgn}(\eta_1) + \dot{\Delta}_V F_V(t) - \xi_2 \end{aligned} \quad (42)$$

2) *Attitude Loop:* Based on the open-loop error system dynamics in (33), the control term $\tau_\Omega(t)$ is designed as:

$$\begin{aligned} \dot{\tau}_\Omega(t) &= -\alpha_\Omega \|\tau_\Omega(t)\| \text{sgn}(\eta_2) - (\alpha_2 + 1)\eta_2 \\ &\quad - \hat{\lambda}_2 \text{sgn}(\eta_2), \end{aligned} \quad (43)$$

where $\alpha_\Omega, \alpha_2 \in \mathbb{R}$ are positive, control gains. $\hat{\lambda}_2 \in \mathbb{R}^3$ is a adaptive nonlinear feedback gain, which is defined as

$$\dot{\hat{\lambda}}_{2i} = \beta_2 \text{sgn}(\eta_2) \eta_2 \quad (44)$$

where $i = 1, 2, 3$; β_2 is a positive adaptation gain.

After substituting (43) into (33), the closed-loop error dynamics is obtained as

$$\begin{aligned} \dot{\eta}_2 &= \tilde{\Gamma}_2 + \Gamma_{2d} - \alpha_\Omega \|\tau_\Omega(t)\| \text{sgn}(\eta_2) - (\alpha_2 + 1)\eta_2 \\ &\quad - \hat{\lambda}_2 \text{sgn}(\eta_2) + \dot{\Delta}_\Omega \tau_\Omega(t) - \xi_4 \end{aligned} \quad (45)$$

IV. STABILITY ANALYSIS

Before providing the stability analysis of the closed-loop quadrotor system, the following conditions, definition and lemma will be utilized in the proof of Theorem 1.

Condition 1 (λ_{ji} -Gain): To facilitate the following stability proof, the adaptive gain λ_{ji} for $j = 1, 2$ and $i = 1, 2, 3$ must satisfy the following condition

$$\lambda_{1i} = \Gamma_{1d} + \frac{1}{k_2} \dot{\Gamma}_{1d}; \quad \lambda_{2i} = \Gamma_{2d} + \frac{1}{k_4} \dot{\Gamma}_{2d} \quad (46)$$

Definition 1: To facilitate the Lyapunov-based proof of Theorem 1, two functions $Q_1(t) \in \mathbb{R}$ and $Q_2(t) \in \mathbb{R}$ are defined as

$$Q_1(t) \triangleq \lambda_1 |\xi_2(0)| - \xi_2^T(0) \Gamma_{1d}(0) - \int_0^t R_1(v) dv \quad (47)$$

$$Q_2(t) \triangleq \lambda_2 |\xi_4(0)| - \xi_4^T(0) \Gamma_{2d}(0) - \int_0^t R_2(v) dv \quad (48)$$

where the auxiliary function $R_1(t) \in \mathbb{R}$ and $R_2(t) \in \mathbb{R}$ are defined as

$$R_1(t) = \eta_1^T(t) [\Gamma_{1d}(t) - \lambda_1 \text{sgn}(\eta_1)] \quad (49)$$

$$R_2(t) = \eta_2^T(t) [\Gamma_{2d}(t) - \lambda_2 \text{sgn}(\eta_2)] \quad (50)$$

Lemma 1: Provided the sufficient conditions in (46) are satisfied, the auxiliary functions in the translational and rotational loop are defined as

$$\int_0^t R_1(v) dv \leq \lambda_1 |\xi_2(0)| - \xi_2^T(0) \Gamma_{1d}(0) \quad (51)$$

$$\int_0^t R_2(v) dv \leq \lambda_2 |\xi_4(0)| - \xi_4^T(0) \Gamma_{2d}(0) \quad (52)$$

Hence, (51) and (52) can be used to prove that $Q_1(t) \geq 0$ and $Q_2(t) \geq 0$. Proof of Lemma 1 can be found in [21] and is omitted here for brevity.

Condition 2 (Control Gain): The control gains defined in (39) and (43) are selected according to the condition

$$\alpha_1 > \frac{\rho^2(\|\mu_1\|)}{4 \min\{(k_1 - \frac{1}{2}), (k_2 - \frac{1}{2}), 1\}} \quad (53)$$

$$\alpha_2 > \frac{\rho^2(\|\mu_2\|)}{4 \min\{(k_3 - \frac{1}{2}), (k_4 - \frac{1}{2}), 1\}} \quad (54)$$

$$\alpha_F \geq \delta_1, \quad \alpha_\tau \geq \delta_2. \quad (55)$$

Theorem 1: For the quadrotor dynamics described in (9a)-(9d) and for a given sufficiently smooth desired trajectory $[x_d, y_d, z_d, \psi_d]^T$, the robust nonlinear control law given in (39) and (43) along with the adaptive parameters updated based on (40) and (44) ensure the tracking error is asymptotically regulated and all the signals remain bounded throughout the closed-loop operation in the sense that

$$\|\xi(t)\| \rightarrow 0 \quad \text{for} \quad t \geq t_n < \infty, \quad (56)$$

where $t_n \in \mathcal{L}_\infty$.

Proof: Let $\mathcal{D} \subset \mathbb{R}^{6n+6+2}$ be a domain containing $w(t) = 0$, where $w(t) \in \mathbb{R}^{6n+1}$ is defined as

$$w(t) \triangleq [\mu^T(t) \quad \tilde{\lambda}_1^T \quad \tilde{\lambda}_2^T \quad \sqrt{Q_1(t)} \quad \sqrt{Q_2(t)}]^T \quad (57)$$

where $\tilde{\lambda}_i = \hat{\lambda}_i - \lambda_i$, ($i = 1, 2$) in (57) represent the difference between the estimated parameter and its true value defined in Condition 1 and $\mu(t) \in \mathbb{R}^{6n}$ is defined as

$$\mu(t) \triangleq [\mu_1^T(t) \quad \mu_2^T(t)]^T, \quad (58)$$

$Q_1(t)$ and $Q_2(t)$ are defined in Definition 1. Let $V(w, t) : \mathcal{D} \times [0, \infty) \rightarrow \mathbb{R}$ be a radially unbounded, positive definite function defined as

$$\begin{aligned} V &= \frac{1}{2} \xi_1^T \xi_1 + \frac{1}{2} \xi_2^T \xi_2 + \frac{1}{2} \xi_3^T \xi_3 + \frac{1}{2} \xi_4^T \xi_4 + \frac{1}{2} \eta_1^T \eta_1 \\ &+ \frac{1}{2} \eta_2^T \eta_2 + Q_1 + Q_2 + \frac{1}{2\beta_1} \tilde{\lambda}_1^T \tilde{\lambda}_1 + \frac{1}{2\beta_2} \tilde{\lambda}_2^T \tilde{\lambda}_2 \end{aligned} \quad (59)$$

which satisfies the inequalities

$$U_1(w) \leq V(w, t) \leq U_2(w), \quad (60)$$

provided the gain Condition 1 are satisfied. In (60), the continuous positive definite functions $U_1(w)$, $U_2(w) \in \mathbb{R}$ are defined as

$$U_1(w) \triangleq \frac{1}{2} \|w\|^2, \quad U_2(w) \triangleq \|w\|^2. \quad (61)$$

After taking the time derivative of (59) and using (12), (13), (24), (25), (42), (45), \dot{V} can be expressed as

$$\begin{aligned} \dot{V} &= \xi_1^T [\xi_2 - k_1 \xi_1] + \xi_2^T [\eta_1 - k_2 \xi_2] + \xi_3^T [\xi_4 - k_3 \xi_3] \\ &+ \xi_4^T [\eta_2 - k_4 \xi_4] + \eta_1^T [\tilde{\Gamma}_1 + \Gamma_{1d} - \alpha_F \|F_V\| \text{sgn}(\eta_1) \\ &- (\alpha_1 + 1) \eta_1 - \hat{\lambda}_1 \text{sgn}(\eta_1) + \dot{\Delta}_V F_V(t) - \xi_2] \\ &+ \eta_2^T [\tilde{\Gamma}_2 + \Gamma_{2d} - \alpha_\Omega \|\tau_\Omega\| \text{sgn}(\eta_2) - (\alpha_2 + 1) \eta_2 \\ &- \hat{\lambda}_2 \text{sgn}(\eta_2) + \dot{\Delta}_\Omega \tau_\Omega(t) - \xi_4] + \dot{Q}_1 + \dot{Q}_2 \\ &+ \frac{1}{\beta_1} \tilde{\lambda}_1^T \dot{\lambda}_1 + \frac{1}{\beta_2} \tilde{\lambda}_2^T \dot{\lambda}_2. \end{aligned} \quad (62)$$

By using the bounding inequalities in (22), (37) and the definition of Q_1, Q_2 from (47), (48), and the definition of $\hat{\lambda}_1, \hat{\lambda}_2$ from (40), (44), the expression in (62) can be upper bounded as

$$\begin{aligned} \dot{V} &\leq \xi_1^T \xi_2 + \xi_3^T \xi_4 - k_1 \|\xi_1\|^2 - k_2 \|\xi_2\|^2 - k_3 \|\xi_3\|^2 \\ &- k_4 \|\xi_4\|^2 + \|\eta_1\| \rho(\|\mu_1\|) \|\mu_1\| + \|\eta_1\| \|\Gamma_{1d}\| \\ &- \|\eta_1\| (\alpha_F) \|F_V\| - (\alpha_1 + 1) \|\eta_1\|^2 - \|\eta_1\| \hat{\lambda}_1 \text{sgn}(\eta_1) \\ &+ \delta_1 \|\eta_1\| \|F_V\| + \|\eta_2\| \rho(\|\mu_2\|) \|\mu_2\| + \|\eta_2\| \|\Gamma_{2d}\| \\ &- \|\eta_2\| (\alpha_\tau) \|\tau_\Omega\| - (\alpha_2 + 1) \|\eta_2\|^2 - \|\eta_2\| \hat{\lambda}_2 \text{sgn}(\eta_2) \\ &+ \delta_2 \|\eta_2\| \|\tau_\Omega\| - \|\eta_1\| \|\Gamma_{1d}\| + \|\eta_1\| \lambda_1 \text{sgn}(\eta_1) \\ &- \|\eta_2\| \|\Gamma_{2d}\| + \|\eta_2\| \lambda_2 \text{sgn}(\eta_2) + \tilde{\lambda}_1^T \text{sgn}(\eta_1) \eta_1 \\ &+ \tilde{\lambda}_2^T \text{sgn}(\eta_2) \eta_2. \end{aligned} \quad (63)$$

But $\xi_1^T \xi_2$ and $\xi_3^T \xi_4$ can be upper bounded as

$$\xi_1^T \xi_2 \leq \frac{1}{2} \|\xi_1\|^2 + \frac{1}{2} \|\xi_2\|^2; \quad \xi_3^T \xi_4 \leq \frac{1}{2} \|\xi_3\|^2 + \frac{1}{2} \|\xi_4\|^2. \quad (64)$$

By using (64), and the gains $\alpha_F, \alpha_\tau, \alpha_1$ and α_2 satisfy the gain condition in Condition 2, the upper bound in (63) can be further simplified as

$$\begin{aligned} \dot{V} &\leq -(k_1 - \frac{1}{2}) \|\xi_1\|^2 - (k_2 - \frac{1}{2}) \|\xi_2\|^2 - \|\eta_1\|^2 \\ &- \alpha_1 \left[\|\eta_1\| - \frac{\rho(\|\mu_1\|)}{2\alpha_1} \|\mu_1\| \right]^2 + \frac{\rho^2(\|\mu_1\|)}{4\alpha_1} \|\mu_1\|^2 \\ &- (k_3 - \frac{1}{2}) \|\xi_3\|^2 - (k_4 - \frac{1}{2}) \|\xi_4\|^2 - \|\eta_2\|^2 \\ &- \alpha_2 \left[\|\eta_2\| - \frac{\rho(\|\mu_2\|)}{2\alpha_2} \|\mu_2\| \right]^2 + \frac{\rho^2(\|\mu_2\|)}{4\alpha_2} \|\mu_2\|^2 \\ &\dot{V} \leq - \left[c_1 - \frac{\rho^2(\|\mu\|)}{4c_2} \right] \|\mu\|^2, \end{aligned} \quad (66)$$

where $c_1 \triangleq \min \left[\min\{(k_1 - \frac{1}{2}), (k_2 - \frac{1}{2}), 1\}, \min\{(k_3 - \frac{1}{2}), (k_4 - \frac{1}{2}), 1\} \right]$ and $c_2 \triangleq \min\{\alpha_1, \alpha_2\}$. The following expression can be obtained from (66)

$$\dot{V} \leq -U(w), \quad (67)$$

where $U(w) = c \|\mu\|^2$, for some positive constant $c \in \mathbb{R}$ is a continuous positive semi-definite function that is defined on the domain

$$\mathcal{K} \triangleq \{w(t) \in \mathbb{R}^{6n+2} \mid \|w\| \leq \rho^{-1} (2\sqrt{c_1 c_2})\}. \quad (68)$$

The expressions in (60) and (66), along with (53), (54) can be used to prove that $V(w, t) \in \mathcal{L}_\infty$ in \mathcal{K} ; hence, $\xi_1(t), \xi_2(t), \xi_3(t), \xi_4(t), \eta_1(t), \eta_2(t) \in \mathcal{L}_\infty$ in \mathcal{K} . Given that $\xi_1(t), \xi_2(t), \xi_3(t), \xi_4(t), \eta_1(t), \eta_2(t) \in \mathcal{L}_\infty$, a standard linear analysis technique can be used along with (13), (15), (25), (27) to show that $\dot{\xi}_1(t), \dot{\xi}_2(t), \dot{\xi}_3(t), \dot{\xi}_4(t) \in \mathcal{L}_\infty$ in \mathcal{K} . Since $\xi_1(t), \xi_2(t), \xi_3(t), \xi_4(t), \eta_1(t), \eta_2(t) \in \mathcal{L}_\infty$, (12) and (24) can be used along with the Assumption 1 to prove that $P(t), V(t) \in \mathcal{L}_\infty$ in \mathcal{K} . Given that $P(t), V(t) \in \mathcal{L}_\infty$, (9a)-(9d) along with Assumption 3 and 4 to prove that the control input $F_V(t), \tau_\Omega(t) \in \mathcal{L}_\infty$ in \mathcal{K} . Since $\eta_1(t), \eta_2(t) \in \mathcal{L}_\infty$, can be used to prove that $\dot{F}_V(t), \dot{\tau}_\Omega \in \mathcal{L}_\infty$ in \mathcal{K} . Given that $\eta_1(t), \eta_2(t), \xi_1(t), \xi_2(t), \xi_3(t), \xi_4(t) \in \mathcal{L}_\infty$, the bounding inequalities in (22), (37) can be used to prove that $\dot{\eta}_1(t), \dot{\eta}_2(t) \in \mathcal{L}_\infty$ in \mathcal{D} . Since $\dot{\xi}_1(t), \dot{\xi}_2(t), \dot{\xi}_3(t), \dot{\xi}_4(t), \dot{\eta}_1(t), \dot{\eta}_2(t) \in \mathcal{L}_\infty$, (23) and (38) can be used to prove that $\mu(t)$ is uniformly continuous in \mathcal{K} . Hence, the definitions of $U(w)$ and $\mu(t)$ can be used to prove that $U(w)$ is uniformly continuous in \mathcal{K} .

Let $\mathcal{S} \subset \mathcal{K}$ denote a set defined as follows:

$$\mathcal{S} \triangleq \left\{ w(t) \in \mathcal{K} \mid U(w(t)) \leq \frac{1}{2} (\rho^{-1} (2\sqrt{c_1 c_2}))^2 \right\}. \quad (69)$$

Theorem 8.4 of [29] can now be invoked to state that

$$c \|\mu(t)\|^2 \rightarrow 0 \quad \text{as} \quad t \rightarrow \infty \quad \forall w(0) \in \mathcal{S}.$$

Based on the definition of $\mu(t)$, (69) can be used to show that

$$\|\xi(t)\| \rightarrow 0 \quad \text{as} \quad t \rightarrow \infty \quad \forall w(0) \in \mathcal{S}. \quad (70)$$

Hence, asymptotic regulation of the quadrotor states is achieved, provided the initial conditions lie within the set \mathcal{S} , where \mathcal{S} can be made arbitrarily large by increasing the control gain α - a semi-global result. ■

V. SIMULATION RESULTS

In this section, numerical examples are illustrated by conducting extensive simulations to validate the efficiency of the proposed adaptive modified RISE control algorithm for both the position and attitude loop with varying magnitudes of the model, actuator uncertainties, and disturbances. During the implementation of the control law in the current numerical simulation, the discontinuous signum function is replaced with the continuously differentiable $\tanh(\cdot)$ function. This is a standard approximation, which relates to the well-accepted definition of an ‘‘equivalent value operator’’ of a discontinuous function [30].

The reader is referred to [25] for a detailed description of the physical parameters, uncertainties, and external disturbance acting on the quadrotor. The simulation results are summarized in Fig.1-6. The results show a comparison between an MRISE-based control formulation in [25] and an

adaptive modified RISE formulation presented in this paper. The comparison is for a specific case, with an uncertainty of 10% deviation from true values and a disturbance magnitude of 5.

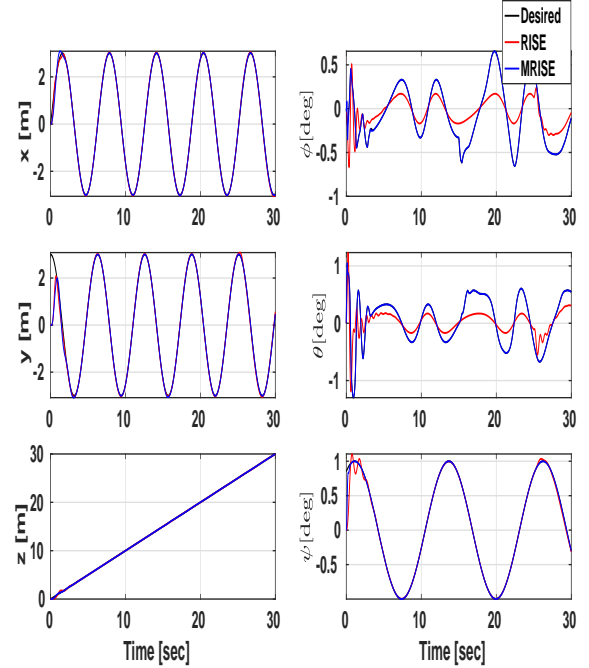


Fig. 1. [Left] Time evolution of the position of the quadrotor, [right] Error between the desired and current state

A minimum snap trajectory proposed in [31] can be utilized to generate feasible trajectories for quadrotors, but in this current work, the desired trajectories are generated using the following definitions

$$[x_{des}, y_{des}, z_{des}, \psi_{des}]^T = [3 \sin(t), 3 \cos(t), t, \sin(t)]^T. \quad (71)$$

The control gains associated with the outer loop in (39) are given as $\alpha_F = 0.01$, $\alpha_1 = 2$, $k_1 = 5$, $k_2 = 2.5$, and those of the inner loop in (43) are given as $\alpha_\tau = 0.01$, $\alpha_2 = 5$, $k_3 = 20$, $k_4 = 9$, respectively.

Fig. 1 shows the positional state $x, y, z, \phi, \theta, \psi$ (blue) of the quadrotor tracking using the control structure presented in this paper, is compared with the quadrotor trajectory (red) using modified RISE-based control in [25] with the desired (black) trajectory defined in (71). The disturbance is introduced at $t = 15$ sec; the proposed adaptive control structure reacted more robustly thereby reducing the error between the current and desired states. Fig 2 shows the corresponding errors associated with the positional states x, y, z during the closed-loop control operation. Fig. 3 shows the tracking error in the translational states of the quadrotor ϕ, θ, ψ orientation during the closed-loop.

Fig. 4 shows the time evolution of the elements of the adaptive parameter estimate $\hat{\lambda}_1$ and $\hat{\lambda}_2$ during closed-loop controller operation. Fig. 5 shows the evolution of the control magnitudes during closed-loop operation. The magnitude of these control signals closely resembles the experimental

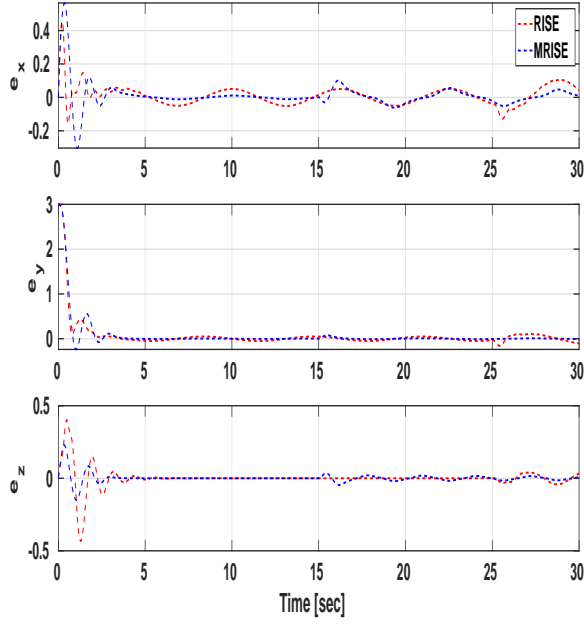


Fig. 2. Time evolution of the error between the desired and measured translational position during the closed loop operation

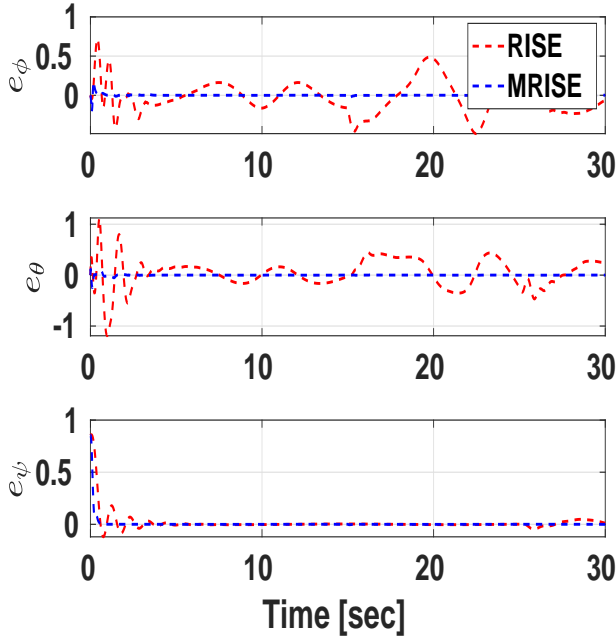


Fig. 3. Time evolution of the error between the desired and measured angular position during the closed loop operation

results presented in [18] for agile trajectory tracking. Fig. 6 shows the bar graph of the mean RMS error in the states P, V, ω, Ω over varying uncertainty levels. The results in Figs.2, 3 and 6 clearly demonstrate the improvement in the closed-loop performance that is achieved by the proposed adaptive modified RISE-based control formulation that compensates under varying levels of model and actuator

uncertainties as well as disturbance magnitudes.

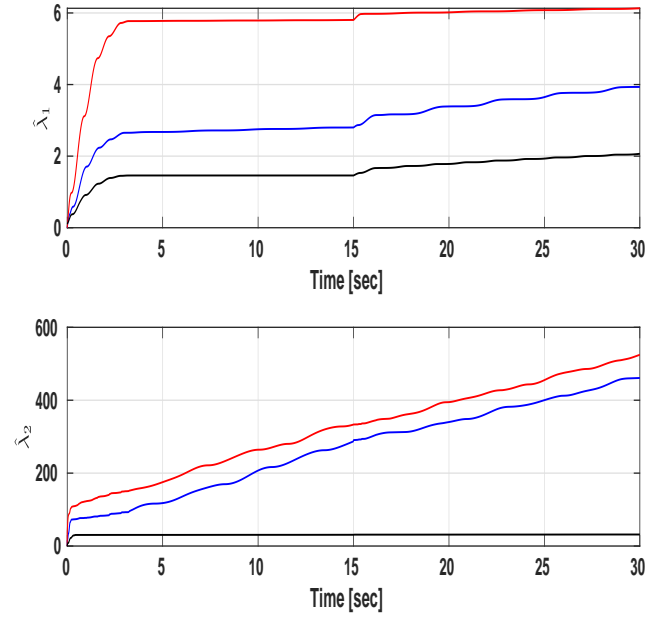


Fig. 4. Time response of the adaptive parameter estimates $\hat{\lambda}_{1i}$ and $\hat{\lambda}_{2i}$

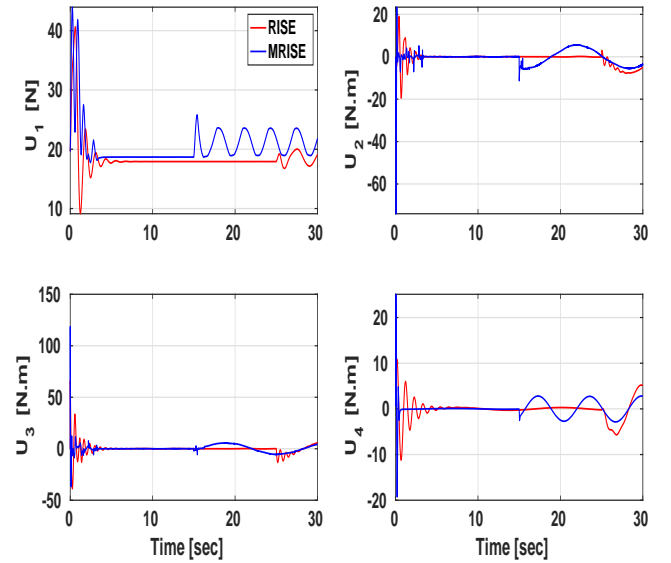


Fig. 5. Commanded control inputs during the closed-loop operation

VI. CONCLUSION

In this paper, an adaptive MRISE state feedback controller is proposed that achieves asymptotic trajectory tracking under gyroscopic effects, model, and actuator uncertainties and at the same time mitigates external disturbances acting on the quadrotor. The proposed nonlinear control algorithms adapt to varying magnitudes of uncertainties, disturbances and

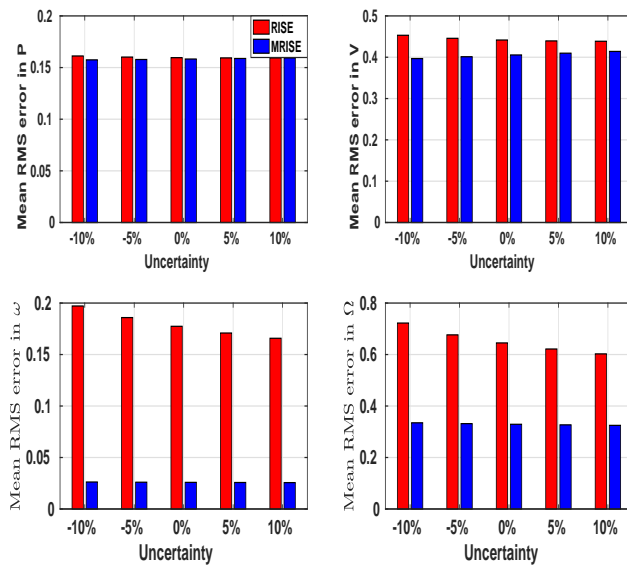


Fig. 6. A bar graph showing the mean RMS error during the closed-loop operation for the states P, V, ω, Ω under varying uncertainty levels

track trajectories of varying speeds. A rigorous Lyapunov-based analysis is utilized to prove asymptotic trajectory tracking of both the position and attitude loops, where the region of convergence can be made arbitrarily large through judicious control gain selection. Detailed numerical simulations are provided to evaluate the proposed control design. Future work will focus on evaluating the proposed robust control methods through real-time experiments on a quadrotor.

REFERENCES

- [1] M. Idrissi, M. Salami, and F. Annaz, "A review of quadrotor unmanned aerial vehicles: applications, architectural design and control algorithms," *Journal of Intelligent & Robotic Systems*, vol. 104, no. 2, p. 22, 2022.
- [2] G. Sonugur, "A review of quadrotor uav: Control and slam methodologies ranging from conventional to innovative approaches," *Robotics and Autonomous Systems*, p. 104342, 2022.
- [3] M. Rinaldi, S. Primatesta, and G. Guglieri, "A comparative study for control of quadrotor uavs," *Applied Sciences*, vol. 13, no. 6, p. 3464, 2023.
- [4] J.-T. Yu, "A unified SO (3) approach to the attitude control design for quadrotors," *IEEE Access*, vol. 9, pp. 64871–64879, 2021.
- [5] M. R. Cohen, K. Abdulrahim, and J. R. Forbes, "Finite-horizon LQR control of quadrotors on $se_2(3)$," *IEEE Robotics and Automation Letters*, vol. 5, no. 4, pp. 5748–5755, 2020.
- [6] R. Miranda-Colorado and L. T. Aguilar, "Robust pid control of quadrotors with power reduction analysis," *ISA transactions*, vol. 98, pp. 47–62, 2020.
- [7] P. Foehn and D. Scaramuzza, "Onboard state dependent lqr for agile quadrotors," in *2018 IEEE International Conference on Robotics and Automation (ICRA)*, pp. 6566–6572, IEEE, 2018.
- [8] L. Martins, C. Cardeira, and P. Oliveira, "Inner-outer feedback linearization for quadrotor control: two-step design and validation," *Nonlinear Dynamics*, vol. 110, no. 1, pp. 479–495, 2022.
- [9] A. Mahmood and Y. Kim, "Decentralized formation flight control of quadcopters using robust feedback linearization," *Journal of the Franklin Institute*, vol. 354, no. 2, pp. 852–871, 2017.
- [10] J. Wang, K. A. Alattas, Y. Bouteraa, O. Mofid, and S. Mobayen, "Adaptive finite-time backstepping control tracker for quadrotor uav with model uncertainty and external disturbance," *Aerospace Science and Technology*, vol. 133, p. 108088, 2023.
- [11] G. Wen, W. Hao, W. Feng, and K. Gao, "Optimized backstepping tracking control using reinforcement learning for quadrotor unmanned aerial vehicle system," *IEEE Transactions on Systems, Man, and Cybernetics: Systems*, vol. 52, no. 8, pp. 5004–5015, 2021.
- [12] Y.-C. Liu and T.-W. Ou, "Non-linear adaptive tracking control for quadrotor aerial robots under uncertain dynamics," *IET Control Theory & Applications*, vol. 15, no. 8, pp. 1126–1139, 2021.
- [13] K. Patnaik and W. Zhang, "Adaptive attitude control for foldable quadrotors," *IEEE Control Systems Letters*, 2023.
- [14] J. Bai, Y. Wang, and H. Xing, "Computational adaptive optimal tracking control of quadrotor uav based on robust control with unknown dynamics," in *2021 33rd Chinese Control and Decision Conference (CCDC)*, pp. 4747–4752, IEEE, 2021.
- [15] D. D. Dhadekar, P. D. Sanghani, K. Mangrulkar, and S. Talole, "Robust control of quadrotor using uncertainty and disturbance estimation," *Journal of Intelligent & Robotic Systems*, vol. 101, pp. 1–21, 2021.
- [16] X. Lin, Y. Wang, and Y. Liu, "Neural-network-based robust terminal sliding-mode control of quadrotor," *Asian Journal of Control*, vol. 24, no. 1, pp. 427–438, 2022.
- [17] J. Baek and M. Kang, "A synthesized sliding-mode control for attitude trajectory tracking of quadrotor uav systems," *IEEE/ASME Transactions on Mechatronics*, 2023.
- [18] J. Jia, K. Guo, X. Yu, L. Guo, and L. Xie, "Agile flight control under multiple disturbances for quadrotor: Algorithms and evaluation," *IEEE Transactions on Aerospace and Electronic Systems*, vol. 58, no. 4, pp. 3049–3062, 2022.
- [19] Z. Li, X. Ma, and Y. Li, "Model-free control of a quadrotor using adaptive proportional derivative-sliding mode control and robust integral of the signum of the error," *International Journal of Advanced Robotic Systems*, vol. 15, no. 5, p. 1729881418800885, 2018.
- [20] L. Yu, G. He, X. Wang, and L. Shen, "A novel fixed-time sliding mode control of quadrotor with experiments and comparisons," *IEEE Control Systems Letters*, vol. 6, pp. 770–775, 2021.
- [21] B. Xian, D. M. Dawson, M. S. de Queiroz, and J. Chen, "A continuous asymptotic tracking control strategy for uncertain nonlinear systems," *IEEE Transactions on Automatic Control*, vol. 49, no. 7, pp. 1206–1211, 2004.
- [22] G. Yang, T. Zhu, F. Yang, L. Cui, and H. Wang, "Output feedback adaptive rise control for uncertain nonlinear systems," *Asian Journal of Control*, vol. 25, no. 1, pp. 433–442, 2023.
- [23] H. Wang, X. Shao, J. Li, and J. Liu, "A velocity-free adaptive rise-based trajectory tracking approach for quadrotors with desired model compensation," *Aerospace Science and Technology*, vol. 92, pp. 551–562, 2019.
- [24] X. Shao, Q. Meng, J. Liu, and H. Wang, "Rise and disturbance compensation based trajectory tracking control for a quadrotor uav without velocity measurements," *Aerospace Science and Technology*, vol. 74, pp. 145–159, 2018.
- [25] K. B. Kidambi, C. Fermüller, Y. Aloimonos, and H. Xu, "Robust nonlinear control-based trajectory tracking for quadrotors under uncertainty," *IEEE Control Systems Letters*, vol. 5, no. 6, pp. 2042–2047, 2020.
- [26] S. Tang and V. Kumar, "Autonomous flight," *Annual Review of Control, Robotics, and Autonomous Systems*, vol. 1, pp. 29–52, 2018.
- [27] R. Mahony, V. Kumar, and P. Corke, "Multirotor aerial vehicles: Modeling, estimation, and control of quadrotor," *IEEE Robotics and Automation magazine*, vol. 19, no. 3, pp. 20–32, 2012.
- [28] J. Svacha, J. Paulos, G. Loianno, and V. Kumar, "Imu-based inertia estimation for a quadrotor using newton-euler dynamics," *IEEE Robotics and Automation Letters*, vol. 5, no. 3, pp. 3861–3867, 2020.
- [29] H. K. Khalil, *Nonlinear control*, vol. 406. Pearson New York, 2015.
- [30] S. V. Drakunov, "Sliding-mode observers based on equivalent control method," in *[1992] Proceedings of the 31st IEEE Conference on Decision and Control*, pp. 2368–2369, IEEE, 1992.
- [31] D. Mellinger and V. Kumar, "Minimum snap trajectory generation and control for quadrotors," in *2011 IEEE international conference on robotics and automation*, pp. 2520–2525, IEEE, 2011.

This figure "Fig1.png" is available in "png" format from:

<http://arxiv.org/ps/2303.10270v1>